Stimulated Raman adiabatic passage in an extended ladder system

Ying-Yu Niu,* Rong Wang, and Ming-Hui Qiu
School of Science, Dalian Jiaotong University, Dalian 116028, China
(Received 11 April 2011; published 10 August 2011)

The rovibrational dynamics of an extended ladder stimulated Raman adiabatic passage (STIRAP) system through permanent dipole moment transitions is investigated theoretically using the time-dependent quantum-wave-packet method for the ground electronic state of the HF molecule. The calculated results show that nearly 100% of the population can be transferred to the target state through (1+2), (1+3), and (2+2) STIRAP schemes. By choosing a suitable excitation pathway, the effects of the background states on the final population of the target state can be removed. For the multiphoton STIRAP process, the one-photon overtone pump scheme is more efficient than the two-photon pump scheme in controlling the population transfer to the target state.

DOI: 10.1103/PhysRevA.84.023406 PACS number(s): 33.80.Be, 42.65.Dr, 33.20.Vq, 33.20.Fb

The manipulation of the population to a prescribed target state with laser pulses has long been a subject of considerable interest [1–5]. The stimulated Raman adiabatic passage (STIRAP) technique has become an important tool for controlling population transfer in both atomic and molecular systems [6–9]. In its simplest three-level system, two counterintuitive pulses are employed. The pump pulse couples the initial and intermediate states and the Stokes pulse couples the intermediate and target states. In this process the two partly overlapping laser pulses can produce a complete population transfer from the initial state to the target state without significant population in the intermediate state.

The extension of the STIRAP system to more complex cases has been proposed theoretically. On the one hand, the three-level systems are extended to multilevel (N-level) systems and the single intermediate state is replaced by $N-2$ intermediate states [10–13]. In most cases, a set of $N-1$ overlapping pulses is employed for N levels. Several multipulse extensions of the STIRAP system to N-level systems have been proposed, such as the alternating STIRAP system [14], in which all the even transitions occur before all the odd transitions, and the straddling STIRAP scheme [15], in which a set of intense pulses corresponding to all intermediate states spans both the Stokes and pump pulses. On the other hand, the conventional (1+1) STIRAP scheme (one-photon pump transition plus one-photon Stokes transition) has been extended to the $(m+n)$ STIRAP scheme (m-photon pump transition plus n-photon Stokes transition) [16–20]. Vrábel and Jakubetz [21] studied the multiphoton STIRAP process using a 28-level system. Utilizing the extended Λ system, they controlled the HCN→HNC isomerization reaction via multiple intermediate states.

In this paper we take the HF molecule, for example, to explore the rovibrational dynamics of the extended ladder STIRAP system in the ground electronic state using the time-dependent quantum-wave-packet method. In our model the multilevel system is described by the rovibrational levels in the ground electronic state and the multiphoton STIRAP process is achieved by the m-photon pump transition and the n-photon Stokes transition. In particular, we investigate numerically the (1+2) STIRAP process including five rovibrational levels, the (1+3) STIRAP process including seven rovibrational levels, and the (2+2) STIRAP process including five rovibrational levels. By choosing suitable intermediate states and transition channels, the extended STIRAP technique can realize a nearly complete population transfer from the initial state to the target state through the permanent dipole moment transitions.

In our theoretical model, only the ground electronic state is taken into account. We assume the initial state to be $|\nu=0, J=0\rangle$ with the magnetic quantum number $M=0$. In the linearly polarized laser field, only the $\Delta M=0$ transition is considered. In the framework of the Born-Oppenheimer approximation, the two-dimensional molecular Hamiltonian including the field-molecule interaction can be expressed as

$$\hat{H} = -\frac{\hbar^2}{2m}\frac{\partial^2}{\partial R^2} + \frac{\hat{J}^2(\theta)}{2mR^2} + V(R) - \mu(R)\cos(\theta)\varepsilon(t), \qquad (1)$$

where m is the reduced mass of the HF molecule, R is the internuclear separation, $\hat{J}$ is the angular momentum operator, and θ is the angle between the molecular axis and the laser electric-field axis. The potential-energy curve $V(R)$ for the ground electronic state is the Morse potential function. The molecular permanent dipole moment $\mu(R)$ is described by the function $\mu(R)=\mu_0 R\exp(-\xi R^4)$. The parameters of the functions $V(R)$ and $\mu(R)$ are adapted from Ref. [22]. The electric field $\varepsilon(t)$ may be composed of two $\sin^2$-shaped pulses,

$$\varepsilon(t) = \sum_{i=P,S} E_i \sin^2\left[\frac{\pi(t-t_{0i})}{\tau_i}\right]\cos[\omega_i(t-t_{0i})], \qquad (2)$$

where t_{0i}, E_i, ω_i, and τ_i are the start time, electric-field amplitude, carrier frequency, and duration of the two pulses, respectively. The subscripts P and S represent the pump and Stokes laser pulses, respectively.

The rovibrational eigenfunction $|\nu, J\rangle$ can be obtained by a direct product of radial and angular eigenfunctions. We use the Legendre polynomial $P_J(\cos\theta)$ as the eigenfunction of the angular part. The radial vibrational function $\phi_{\nu,J}(R)$ is obtained by solving numerically the one-dimensional time-independent Schrödinger equation

$$\left[-\frac{\hbar^2}{2m}\frac{\partial^2}{\partial R^2} + \frac{J(J+1)\hbar^2}{2mR^2} + V(R)\right]\phi_{\nu,J}(R) = \epsilon_{\nu,J}\phi_{\nu,J}(R). \qquad (3)$$

*niuyy@djtu.edu.cn

Equation (3) can be solved by the Fourier grid Hamiltonian method [23].

Using the split operator method [24], information on the nuclear dynamics can be obtained for a given initial condition. By projecting the total wave function $\Psi(t)$ onto the rovibrational eigenstates $|v,J\rangle$, one can compute the time-dependent population of the rovibrational levels

$$P_{v,J}(t) = |\langle v,J|\Psi(t)\rangle|^2. \quad (4)$$

We first consider a case of the (1+2) STIRAP transition in which the initial rovibrational state is $|0,0\rangle$; the intermediate states are $|2,1\rangle$, $|3,0\rangle$, and $|3,2\rangle$; and the target state is $|4,1\rangle$. In this process, the pump pulse drives the one-photon overtone transition and the Stokes pulse drives the two-photon transition

$$\begin{aligned} |0,0\rangle &\rightarrow (\text{one-photon overtone pump}) \rightarrow |2,1\rangle \\ &\rightarrow (\text{one-photon Stokes}) \\ &\rightarrow \left\{ \begin{matrix} |3,0\rangle \\ |3,2\rangle \end{matrix} \right\} \rightarrow (\text{one-photon Stokes}) \rightarrow |4,1\rangle. \quad (5) \end{aligned}$$

Figure 1 shows the population dynamics controlled by the two counterintuitive pulses. The laser parameters of the two pulses are shown in Fig. 1 (b). The overlapping time of the two pulses is 1.888 ps. In Figs. 1(a) and 1(b) the Stokes pulse causes the population curve of the initial state to oscillate slightly before the pump pulse is turned on ($t <$ 0.975 ps). When the intensity of the Stokes pulse reaches about 30 MV cm^{-1} ($t = 1.25$ ps), a small amount of the population can be found in the target and intermediate states. With the time evolution, the population of the initial state decreases to 0.15% and the population of the target state increases to 98.41%. Figures 1(c)–1(e) show the populations of the three intermediate states. The maximal populations of the three intermediate states are about 0.146, 0.110, 0.017 and the final populations at the end of the two pulses are 0.0093, 0.0042, 0, respectively. In the excitation pathway [Eq. (5)], the Stokes pulse induces the transition from the state $|2,1\rangle$ to the state $|4,1\rangle$ through two transitions. For the transition $|2,1\rangle \rightarrow |3,0\rangle \rightarrow |4,1\rangle$, the one-photon detunings of the Stokes pulse from its respective transition frequencies are 54.80 and 44.24 cm^{-1}. For the transition $|2,1\rangle \rightarrow |3,2\rangle \rightarrow |4,1\rangle$, the one-photon detunings are 166.30 and 155.75 cm^{-1}, which are larger than those for the transition $|2,1\rangle \rightarrow |3,0\rangle \rightarrow |4,1\rangle$. Therefore, most population transfer takes place via the state $|3,0\rangle$ and the maximal population of the state $|3,0\rangle$ is larger than that of the state $|3,2\rangle$.

In Fig. 1(a) the population curves display obvious oscillatory behavior, which illustrates that population transfer to and fro takes place in the initial, target, intermediate, and background states. Lan *et al.* [25] illustrated that the background states may divert significant amounts of population away from the target state under suitable conditions. In our ladder system for the HF molecule, the two partly overlapping pulses can produce other excitation routes such as $|2,1\rangle \rightleftarrows |1,0\rangle \rightleftarrows |0,1\rangle$, $|2,1\rangle \rightleftarrows |4,0\rangle$, and $|2,1\rangle \rightleftarrows |4,2\rangle$. Although these background states enhance the oscillatory behavior of the population curves in Fig. 1(a), their final populations are zero at the end of the two pulses, i.e., the final population of the target state is not affected by the background states. Figure 1(f) shows the time-dependent energy of the wave function. Different from the population curves, the energy curve smoothly increases from -0.2157 cm^{-1} (the eigenenergy of the initial state) to -0.1486 cm^{-1} (the eigenenergy of the target state).

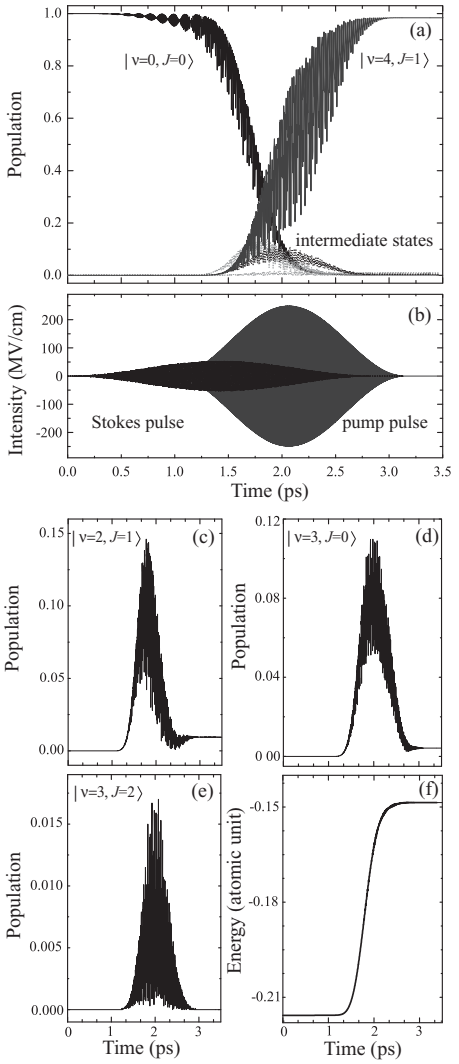

FIG. 1. Complete population transfer for the (1+2) STIRAP transition (one-photon overtone pump transition plus two-photon Stokes transition). (a) Time-dependent populations in the initial, intermediate, and target states. (b) Pump and Stokes pulses with a counterintuitive sequence: $E_P = 248.63$ MV cm^{-1}, $\omega_P = 7791.00$ cm^{-1}, $\tau_P = 2.176$ ps, $t_{0P} = 0.975$ ps, $E_S = 52.71$ MV cm^{-1}, $\omega_S = 3524.76$ cm^{-1}, $\tau_S = 2.863$ ps, and $t_{0S} = 0$ ps. (c)–(e) Time-dependent populations in the three intermediate states. (f) Time-dependent energy of the wave function.

Figure 2(a) shows time-dependent populations for the (1+3) STIRAP process in which the initial rovibrational state is $|0,0\rangle$ and the target state is $|5,2\rangle$. The five intermediate states are $|2,1\rangle$, $|3,0\rangle$, $|3,2\rangle$, $|4,1\rangle$, and $|4,3\rangle$. This transition is the O branch of the Ramam transition ($\Delta J = 2$). The excitation pathway is as follow:

$$\begin{aligned} |0,0\rangle &\rightarrow (\text{one-photon overtone pump}) \rightarrow |2,1\rangle \\ &\rightarrow (\text{one-photon Stokes}) \end{aligned}$$

$$\rightarrow \left\{ \begin{array}{l} |3,0\rangle \rightarrow \text{(one-photon Stokes)} \rightarrow |4,1\rangle \\ |3,2\rangle \rightarrow \text{(one-photon Stokes)} \rightarrow \left\{ \begin{array}{l} |4,1\rangle \\ |4,3\rangle \end{array} \right. \end{array} \right\}$$
$$\rightarrow \text{(one-photon Stokes)} \rightarrow |5,2\rangle. \quad (6)$$

In Fig. 2 the final populations of the states $|0,0\rangle$ and $|5,2\rangle$ are 0.40% and 98.63%, respectively, and the maximal populations of the five intermediate states are about 0.133, 0.052, 0.019, 0.066, and 0.028. The overlapping time of the two pulses is 2.429 ps and the amplitude of the Stokes pulse is 97.96 MV cm^{-1}. Compared with the above (1+2) STIRAP scheme, the overlapping time is longer by about 28% and the amplitude of three-photon Stokes pulse is larger by about 85%. For the transition $|0,0\rangle \rightarrow |2,1\rangle$, the optimal frequency of the pump pulse is 7766.20 cm^{-1} and the corresponding one-photon detuning is 28.76 cm^{-1}. If the frequency of the pump pulse is chosen as the resonance frequency 7794.96 cm^{-1}, a large amount of population can be transferred to the background state $|9,0\rangle$ through the transition $|5,2\rangle \rightarrow |6,1\rangle \rightarrow |9,0\rangle$. When the two pulses are over, about 15% of the population stays in the state $|9,0\rangle$, which reduces the final population of the target state. In the excitation pathway [Eq. (6)], the three-photon Stokes transition comprises four intermediate states. The one-photon detunings for the transitions $|2,1\rangle \rightarrow |3,0\rangle$ and $|3,0\rangle \rightarrow |4,1\rangle$ are 111.55 and 12.51 cm^{-1}. For the transitions $|2,1\rangle \rightarrow |3,2\rangle$, $|3,2\rangle \rightarrow |4,1\rangle$, and $|3,2\rangle \rightarrow |4,3\rangle$, the detunings are 223.05, 98.99, and 79.73 cm^{-1}, respectively. It can be seen that most of the population in the target state is from the transition $|2,1\rangle \rightarrow |3,0\rangle \rightarrow |4,1\rangle \rightarrow |5,2\rangle$, which results in the maximal populations of the states $|3,0\rangle$ and $|4,1\rangle$ being larger than those of the states $|3,2\rangle$ and $|4,3\rangle$.

We have calculated the (1+4) STIRAP scheme (one-photon overtone pump transition plus four-photon Stokes transition) for controlling population to $|\nu = 6\rangle$. In this process the presence of too many intermediate states increases the effects of the background states on population transfer and the final population of the target state is decreased. Figure 3 shows population transfer from the initial state $|0,0\rangle$ to the target state $|6,1\rangle$ through the (1+2) STIRAP scheme. The excitation pathway is as follow:

$$|0,0\rangle \rightarrow \text{(one-photon overtone pump)} \rightarrow |2,1\rangle$$
$$\rightarrow \text{(one-photon overtone Stokes)}$$
$$\rightarrow \left\{ \begin{array}{l} |4,0\rangle \\ |4,2\rangle \end{array} \right\} \rightarrow \text{(one-photon overtone Stokes)} \rightarrow |6,1\rangle. \quad (7)$$

In Fig. 3 the final populations of the initial and target states are 0.94% and 98.48%, respectively, and the maximal populations of the three intermediate states are about 0.143, 0.030, and 0.018. The overlapping time and the total duration of the two pulses are 3.031 and 5.514 ps, respectively, which are longer than those in the two preceding cases. The amplitude of the Stokes pulse for the two-photon overtone transition is 198.23 MV cm^{-1}, which is two times larger than that for the three-photon transition. The stronger Stokes pulse enhances the oscillatory behavior of the target-state population in Fig. 3(a).

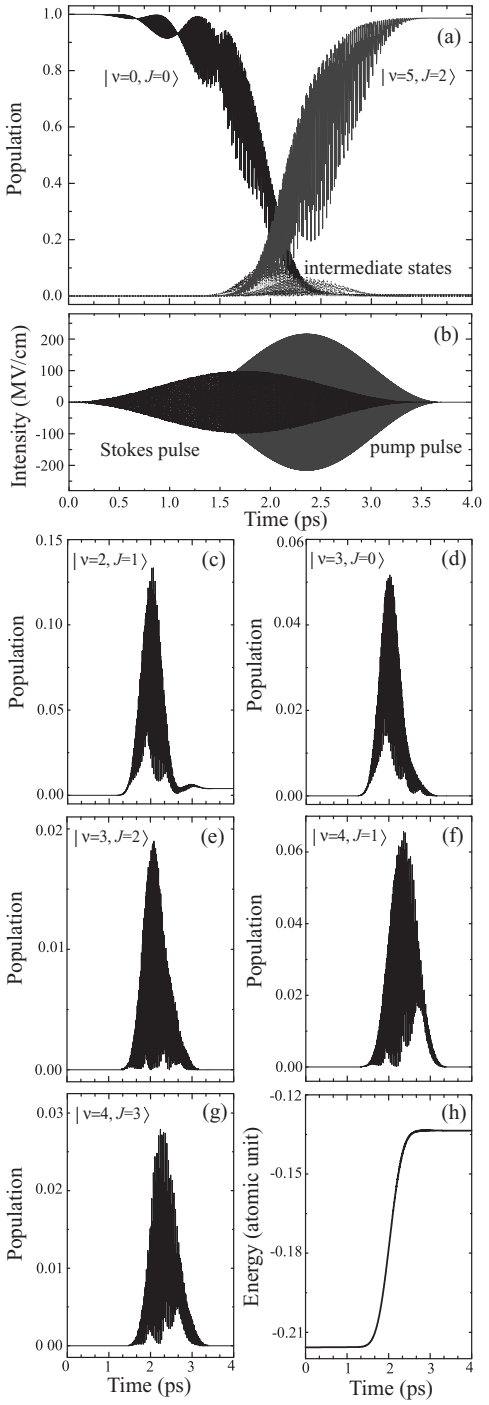

FIG. 2. Complete population transfer for the (1+3) STIRAP transition (one-photon overtone pump transition plus three-photon Stokes transition). (a) Time-dependent populations in the initial, intermediate, and target states. (b) Pump and Stokes pulses with a counterintuitive sequence: $E_P = 216.00$ MV cm^{-1}, $\omega_P = 7766.20$ cm^{-1}, $\tau_P = 2.655$ ps, $t_{0P} = 1.033$ ps, $E_S = 97.96$ MV cm^{-1}, $\omega_S = 3468.01$ cm^{-1}, $\tau_S = 3.462$ ps, and $t_{0S} = 0$ ps. (c)–(g) Time-dependent populations in the five intermediate states. (h) Time-dependent energy of the wave function.

In preceding discussion, population transfer from the state $|\nu = 0\rangle$ to the state $|\nu = 2\rangle$ takes place through the one-photon

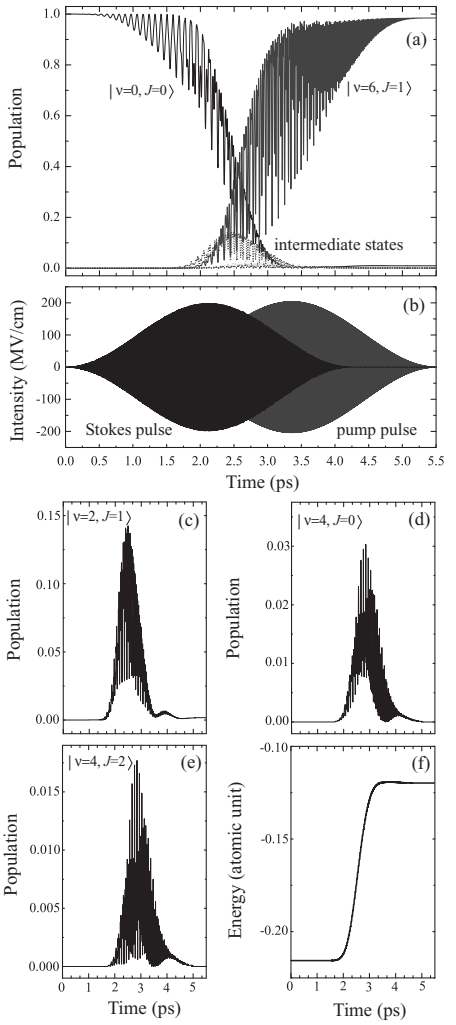

FIG. 3. Complete population transfer for the (1+2) STIRAP transition (one-photon overtone pump transition plus two-photon overtone Stokes transition). (a) Time-dependent populations in the initial, intermediate, and target states. (b) Pump and Stokes pulses with a counterintuitive sequence: $E_P = 203.89$ MV cm^{-1}, $\omega_P = 7787.05$ cm^{-1}, $\tau_P = 4.309$ ps, $t_{0P} = 1.205$ ps, $E_S = 198.23$ MV cm^{-1}, $\omega_S = 6707.64$ cm^{-1}, $\tau_S = 4.236$ ps, and $t_{0S} = 0$ ps. (c)–(e) Time-dependent populations in the three intermediate states. (f) Time-dependent energy of the wave function.

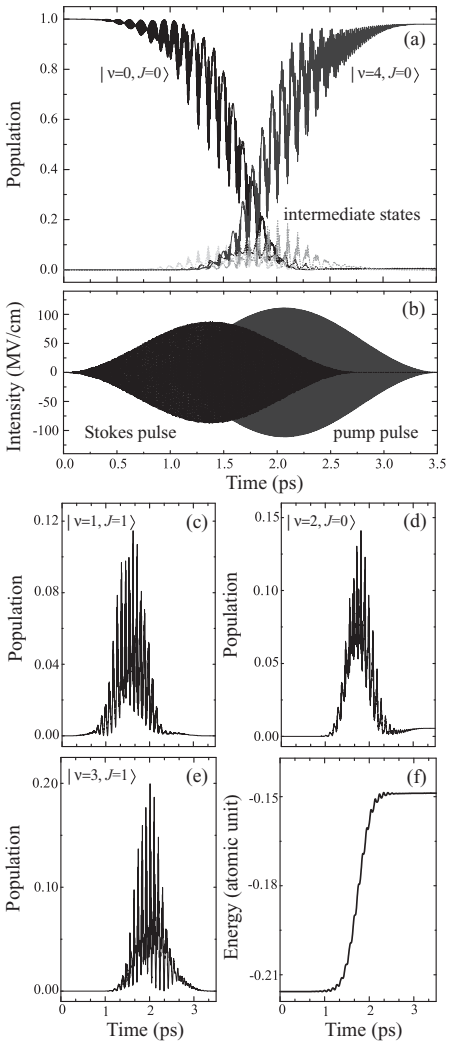

FIG. 4. Complete population transfer for the (2+2) STIRAP transition (two-photon pump transition plus two-photon Stokes transition). (a) Time-dependent populations in the initial, intermediate, and target states. (b) Pump and Stokes pulses with a counterintuitive sequence: $E_P = 110.92$ MV cm^{-1}, $\omega_P = 3885.89$ cm^{-1}, $\tau_P = 2.882$ ps, $t_{0P} = 0.629$ ps, $E_S = 87.15$ MV cm^{-1}, $\omega_S = 3525.71$ cm^{-1}, $\tau_S = 2.751$ ps, and $t_{0S} = 0$ ps. (c)–(e) Time-dependent populations in the three intermediate states. (f) Time-dependent energy of the wave function.

overtone transition. This process can be replaced by the two-photon transition. Figure 4 shows time-dependent populations for the (2+2) STIRAP process in which the target state is $|4,0\rangle$. In this transition process $\Delta J = 0$ corresponds to the Q branch of the Ramam transition and population transfer is achieved according to the excitation pathway

$$|0,0\rangle \rightarrow \text{(one-photon pump)} \rightarrow |1,1\rangle \rightarrow \text{(one-photon pump)} \rightarrow |2,0\rangle \rightarrow \text{(one-photon Stokes)} \rightarrow |3,1\rangle \rightarrow \text{(one-photon Stokes)} \rightarrow |4,0\rangle. \quad (8)$$

In Fig. 4 the final populations of the initial and target states are 0.43% and 98.01%, respectively, and the maximal populations of the intermediate states are about 0.115, 0.141, and 0.200. The overlapping time of the two pulses is 2.122 ps and the amplitude of the pump pulse for the two-photon transition is 110.92 MV cm^{-1}, which is smaller than that for the one-photon overtone transition. In the three preceding cases, the intermediate and target states get populated at nearly the same time. In Fig. 4(a) the intermediate state $|1,1\rangle$ gets populated at $t = 0.85$ ps and the target state gets populated at $t = 1.22$ ps. For the (2+2) STIRAP scheme, the pump pulse can produce the transition $|1,1\rangle \rightleftarrows |2,2\rangle$, which provides more excitation routes for background states such as $|2,2\rangle \rightleftarrows |3,3\rangle \rightleftarrows |2,4\rangle$, $|2,2\rangle \rightleftarrows |3,3\rangle \rightleftarrows |4,4\rangle \rightleftarrows |5,3\rangle$, and $|2,2\rangle \rightleftarrows |1,3\rangle \rightleftarrows |0,2\rangle$. The population transfer among the initial, target, intermediate, and background states causes a slight oscillatory behavior of the energy curve in Fig. 4(f). We calculate the (2+3) STIRAP scheme for controlling population transfer to the target state $|5,1\rangle$. The results show that 3.12% of the population stays in

the background states and the maximal populations of the intermediate states reach about 0.253. Compared with the one-photon overtone pump scheme, the maximal populations of the intermediate states for the two-photon pump scheme are larger and the background states have more effects on the STIRAP process.

In conclusion, we have studied the rovibrational dynamics of the extended ladder STIRAP system, with the HF molecule as the example. The calculated results show that nearly 100% of the population can be transferred to the target state through the extended ladder STIRAP system. The background states can enhance the oscillatory behavior of the population curves and reduce the final population of the target state. By choosing a suitable excitation pathway, the effects of the background states on the final population of the target state can be removed. For the multiphoton STIRAP process, the one-photon overtone pump scheme is more efficient than the two-photon pump scheme in controlling population transfer to the target state.

This work was supported by the National Science Foundation of China under Grant No. 11047177 and the Education Department of Liaoning Province under Grant No. 2009A131.

[1] M. V. Korolkov, G. K. Paramonov, and B. Schmidt, J. Chem. Phys. **105**, 1862 (1996).
[2] B. M. Garraway and K. A. Suominen, Phys. Rev. Lett. **80**, 932 (1998).
[3] B. J. Sussman, D. Townsend, M. Y. Ivanov, and A. Stolow, Science **314**, 278 (2006).
[4] E. A. Shapiro, A. Péer, J. Ye, and M. Shapiro, Phys. Rev. Lett. **101**, 023601 (2008).
[5] S. A. Malinovskaya and V. S. Malinovsky, Opt. Lett. **32**, 707 (2007).
[6] G. Gaubatz, P. Rudecki, S. Schiemann, and K. Bergmann, J. Chem. Phys. **92**, 5363 (1990).
[7] Y.-Y. Niu, R. Wang, and M.-H. Qiu, Phys. Rev. A **81**, 043406 (2010).
[8] N. V. Vitanov and B. W. Shore, Phys. Rev. A **73**, 053402 (2006).
[9] H. T. K. Bergmann and B. W. Shore, Rev. Mod. Phys. **70**, 1003 (1998).
[10] Y. B. Band and P. S. Julienne, J. Chem. Phys. **95**, 5681 (1991).
[11] B. W. Shore, J. Martin, M. P. Fewell, and K. Bergmann, Phys. Rev. A **52**, 566 (1995).
[12] T. Nakajima, Phys. Rev. A **59**, 559 (1999).
[13] I. R. Solá, V. S. Malinovsky, and D. J. Tannor, Phys. Rev. A **60**, 3081 (1999).
[14] B. W. Shore, K. Bergmann, J. Oreg, and S. Rosenwaks, Phys. Rev. A **44**, 7442 (1991).
[15] V. S. Malinovsky and D. J. Tannor, Phys. Rev. A **56**, 4929 (1997).
[16] L. P. Yatsenko, S. Guérin, T. Halfmann, K. Böhmer, B. W. Shore, and K. Bergmann, Phys. Rev. A **58**, 4683 (1998).
[17] C. A. Marx and W. Jakubetz, J. Chem. Phys. **125**, 234103 (2006).
[18] S. Guérin, L. P. Yatsenko, and H. R. Jauslin, Phys. Rev. A **63**, 031403(R) (2001).
[19] S. Guérin, L. P. Yatsenko, T. Halfmann, B. W. Shore, and K. Bergmann, Phys. Rev. A **58**, 4691 (1998).
[20] K. Böhmer, T. Halfmann, L. P. Yatsenko, B. W. Shore, and K. Bergmann, Phys. Rev. A **64**, 023404 (2001).
[21] I. Vrábel and W. Jakubetz, J. Chem. Phys. **118**, 7366 (2003).
[22] I. V. Andrianov and G. K. Paramonov, Phys. Rev. A **59**, 2134 (1999).
[23] C. C. Marston and G. G. Balint-Kurti, J. Chem. Phys. **91**, 3571 (1989).
[24] M. D. Feit, J. A. Fleck Jr., and A. Steiger, J. Comput. Phys. **47**, 412 (1982).
[25] B.-L. Lan, I. Vrábel, and W. Jakubetz, J. Chem. Phys. **121**, 10401 (2004).